JOURNAL OF NANO- AND ELECTRONIC PHYSICS
Vol. **8** No 2, 02055(5pp) (2016)

ЖУРНАЛ НАНО- ТА ЕЛЕКТРОННОЇ ФІЗИКИ
Том **8** № 2, 02055(5cc) (2016)

Structure and Optical Properties of Polycrystalline $In_xSb_{30-x}Se_{70}$ ($0 \le x \le 25$) Chalcogenide Alloys

Shaveta Sharma[1], Rita Sharma[1], Praveen Kumar[2], R. Chander[1], R. Thangaraj[1], M. Mian[1]

[1] *Semiconductors Laboratory, Department of Physics, GND University, Amritsar 143005, India*
[2] *Department of Physics, DAV University, Sarmastpur, Jalandhar-144012, India*

(Received 12 January 2016; revised manuscript received 11 June 2016; published online 21 June 2016)

The spectroscopic studies of various physical properties of glassy and polycrystalline chalcogenide alloys are important due to their importance as active materials in various solid state devices. The composition dependence of these properties are explained on the basis of coordination number, but the splitting of this effect from the nature of additive is imperative for furthering the understanding of these systems. In the present work, the structural and spectroscopic investigations of melt quenched bulk In-Sb-Se chalcogenide alloys have been studied by XRD, RAMAN and optical spectroscopic techniques. The XRD study reveals the polycrystalline nature of the samples. The composition was analysed using the energy dispersive X-ray spectroscopy technique. The XRD study reveals the crystallization of Sb_2Se_3 and β-In_2Se_3 phases while the increase in the intensity for *β*-In_2Se_3 phase has been observed with the increase in indium content. The RAMAN spectra also reveal the formation of chalcogenide based Sb and In structural units. The diffused reflectance spectrum was used to calculate the optical absorption in 800-1500 nm spectral region and used to study the composition dependence of the optical gap in these samples. The results have been discussed in conjunction with the heterogeneous phases; density of defect states; electronegativity and average mean bond energy for these polycrystalline alloys.

Keywords: Chalcogenide alloys, XRD, Optical property, Raman spectroscopy.

DOI: 10.21272/jnep.8(2).02055 PACS numbers: 78.30.Ly, 78.40.Fy, 71.23.Cq

1. INTRODUCTION

Chalcogenide glasses and alloys are very prodigious class of semiconductor materials because of their potential use in optoelectronics, microelectronics, electro photography, photo-resist, holographic, solar cells etc. [1]. The presence of various defect states, their density and distribution in the mobility gap plays an important role for the suitability of the material w.r.t. devices. Also, when the average coordination number ($\langle r \rangle$) approaches certain value, various physical properties such as mechanical, thermal, electrical and optical properties find unique behaviour [2-4]. Two types of percolation thresholds viz. Rigid percolation threshold (RPT) at $\langle r \rangle = 2.40$ proposed by Thorpe, where the network undergoes phase transition from elastically floppy to the stressed-rigid state which optimizing the good glass-forming tendency [5]. The other type of threshold is Chemical Threshold (CT), according to which there exists a composition having maximum number of heteropolar bonds in the system and behaves as least constrained [6]. In the IV-V-VI glassy system, CT occur between $\langle r \rangle = 2.40$ to 2.67 [7] and generally many of the composition dependent properties for these network systems are greatly elaborated on their dependence on the $\langle r \rangle$ only. In order to improve the glass forming area III-IV-VI glassy system, the elements having light atomic masses, short atomic radii, large number of lone pairs, high degree of covalent bonds etc. were added to chalcogens [8]. As the physical properties of chalcogenide system depends both on composition and nature of additive in the parent system. There are glassy alloys having same $\langle r \rangle$ for different compositions of a system or by isoelectronic substitution for furthering the complete knowledge of this special class of chalcogenide glasses and alloys. The alloys belonging to Sb-Se binary system exhibits switching effect, photoconductivity, photovoltaic and thermoelectric properties for their potential applications as absorber layer in the solar cells and optoelectronic devices etc. due to enhancement in the properties of Se upon alloying [9-10]. The phenomena of charge trapping, transport properties, relation between the band gap and composition of Se-Sb have been well reported in the literature [11-13]. The addition of third element to Se-Sb causes, structural changes which modifies the glass forming area, creates compositional and configurational disorder, band structure and various physical parameters [14-16].

In the present work, we have studied the effect of substitution of Sb by In in the $In_xSb_{30-x}Se_{70}$ ($0 \le x \le 25$) chalcogenide system having average coordination number ($\langle r \rangle = 2.3$) which is less than 2.40 and the system belongs to floppy network.The structural and optical properties are studied by using the X-ray diffraction, RAMAN spectroscopy and UV-Vis absorption studies.

2. EXPERIMENTAL DETAILS

Bulk samples of $In_xSb_{30-x}Se_{70}$ ($0 \le x \le 25$) were prepared by using conventional melt quenching technique. Appropriate amount of the constituent elements with 5N purity were weighed and then sealed in pre-cleaned quartz ampoules having inner-diameter 0.4 cm and length ~10 cm under vacuum at 10^{-5} mbar. These were heated in a furnace at 800 °C for 48 hours and periodically rocked for ensuring the homogenous mixing of constituent elements. Finally, the ampoules are air quenched and the samples were extracted by etching the quartz ampoules by HF solution. These bulk samples were finely grounded and used for various charac-

terizations.

The amorphous/crystalline phases of bulk synthesized samples were studied using X-ray diffractometer (D8 Focus, Bruker, Germany) with Cu k_α line ($\lambda = 0.154$ nm) operated at 35 kV and 30 mA. Crystalline phases for all compositions were identified with standard PCPDF database. Chemical composition were studied by EDX (Oxford Instrument) equipped with FESEM (Supra 55, Carl Zeiss). Raman spectral studies were performed on "RenishawInVia Reflex Micro Raman Spectrometer" using wavelength 514 nm with Ar Ion Laser (5 mW), and 2400 lines/mm diffraction grating having suitable filter. Measurements were done in an un-polarised mode at room temperature in back scattering at a spectral resolution of 1.0 cm^{-1}. Diffuse reflectance measurements were carried out by using UV-Vis-NIR spectrophotometer (UV-3600, Shimadzu, Japan).

3. RESULTS AND DISCUSSION

3.1 Crystalline Phases and Composition

Figure 1 shows the X-ray diffraction patterns for as-prepared bulk $In_xSb_{30-x}Se_{70}$ ($0 \le x \le 25$) samples. Sharp diffraction peaks reveal the polycrystalline character and the two crystalline phases viz. orthorhombic phase of $Sb_2Se_3$and rhombohedral phase of β-In_2Se_3 (PCPDF cards: 75-1462 and 35-1056 respectively) are found to exit in $In_xSb_{30-x}Se_{70}$ system. It is found that the majority phase crystallizes to orthorhombic phase of Sb_2Se_3 without any indication of the crystallization of the remnant Se in the parent$Sb_{30}Se_{70}$ alloy. The addition of small concentrations of In ($x = 5$) yields the crystallization of new phase corresponding to β-In_2Se_3at positions 18.80º, 30.23º, 48.17º, 49.51º, 58.56º. The intensity of the peaks corresponding to this phase has been found to dominate with further increase in indium content. Since the difference in the structure of crystalline phases of the binaries and the growth of In-phase even at small concentrations suggest that In does not go into the lattice positions of the orthorhombic Sb_2Se_3 phase. The inclusion of higher amounts of indium thus favours the formation of heterogeneous phases and increased crystallinity with the relatively dominant peaks for β-In_2Se_3 phase in the bulk alloys and Sb_2Se_3phase correspondingly decreases.

The elemental composition of each bulk samples was determined by energy dispersive X-ray spectroscopy (EDS) and figure 2 shows the EDS spectra for the $Se_{70}Sb_{30}$ alloy. The atomic percentage of all the elements present in the as-prepared bulk samples are tabulated in Table 1. These results suggest that the as-prepared samples are nearly stoichiometric with those compositions used for the synthesis of the samples.

3.2 Raman Analysis

Raman spectral studies enable probing of the local vibrational modes of the network glasses and alloys, which provides the information about the atomic structures complementary to XRD studies. Figure 3 shows the Raman spectrum for $In_xSb_{30-x}Se_{70}$ ($0 \le x \le 25$) chalcogenide alloys. Raman spectrum of as-prepared $Sb_{30}Se_{70}$ exhibits five bands: two dominant peaks at 188 and 250 cm^{-1} and three weak peaks at ~112, 210, and 369 cm^{-1}.

The Raman vibrational modes for Se has been assigned in two spectral regions, one is bond-bending (70-150 cm^{-1}) and another is bond stretching (200-300 cm^{-1}) [17]. The main Raman band at 250 cm^{-1} can be ascribed to the eight membered Se_8 rings [18-19]. The observation of feeble peaks at ~ 112 cm^{-1} and 369 cm^{-1} can be ascribed to the bond bending modes of the Se and found to vanish for further composition due

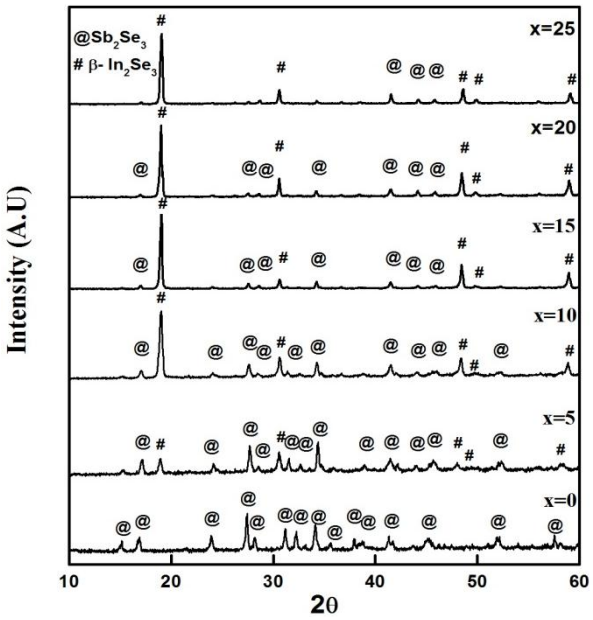

Fig. 1 – X-ray diffraction patterns for as-prepared bulk $In_xSb_{30-x}Se_{70}$ ($0 \le x \le 25$) chalcogenide alloys

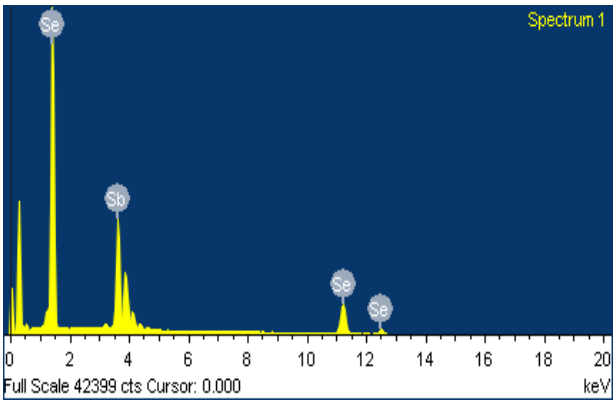

Fig. 2 – EDS spectra of $Se_{70}Sb_{30}$ chalcogenide alloys

Table 1 – Elemental compositions of as-prepared bulk $In_xSb_{30-x}Se_{70}$ ($0 \le x \le 25$) alloys

Sample	Compositions (at. %)		
	Se	Sb	In
$Se_{70}Sb_{30}$	67.28	32.72	0.00
$Se_{70}Sb_{25}In_5$	71.79	23.05	5.16
$Se_{70}Sb_{20}In_{10}$	69.73	16.51	13.76
$Se_{70}Sb_{15}In_{15}$	69.36	11.57	19.07
$Se_{70}Sb_{10}In_{20}$	70.46	7.73	21.81
$Se_{70}Sb_5In_{25}$	70.44	4.32	25.24

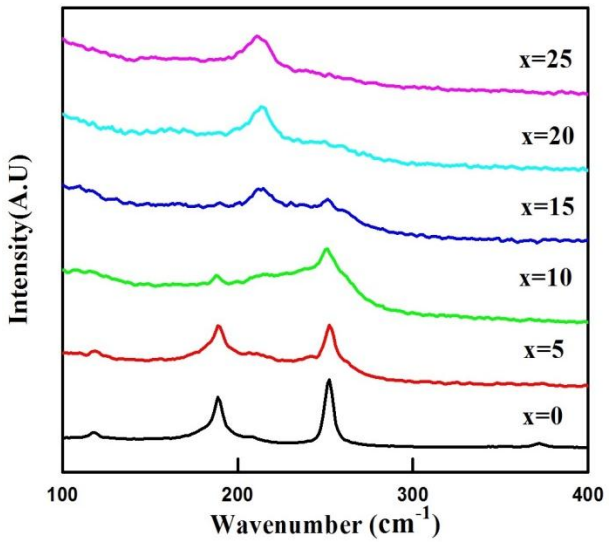

Fig. 3 – Raman spectra for as-prepared bulk $In_xSb_{30-x}Se_{70}$ ($0 \le x \le 25$) chalcogenide alloys

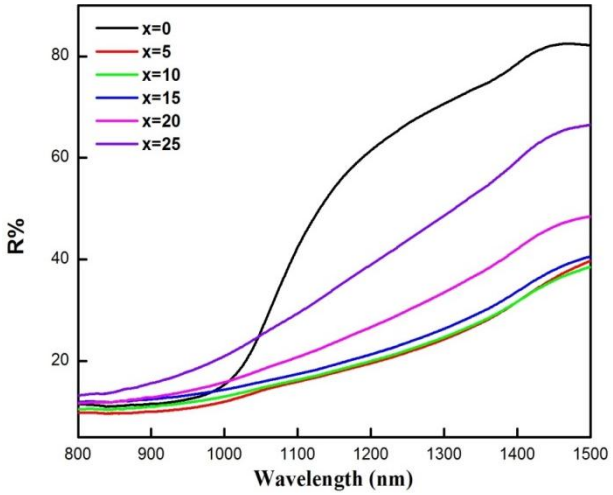

Fig. 4 – Reflectance spectra of as-prepared bulk $In_xSb_{30-x}Se_{70}$ ($0 \le x \le 25$) chalcogenide alloys

Table 2 – Various optical parameters such as optical gap (E_0) and tailing parameter (B^{-1}) for as-prepared $In_xSb_{30-x}Se_{70}$ ($0 \le x \le 25$) chalcogenide alloys

Sample (x)	E_0 (± 0.01 eV)	B^{-1} (± 0.06 × 10^{-5} cm^{-1} eV^{-1})
0	1.18	412.8
5	1.09	472.8
10	1.07	627.9
15	1.05	911.1
20	1.12	918.7
25	1.19	924.3

to contraction of interatomic bonds with the breaking of Se chains by either Sb or In [17, 20]. One another weak peak at ~ 210 cm^{-1} can be ascribed from either Se-Se chain bond or asymmetrical stretching of pyramidal $SbSe_3$ mode [21]. The broad band at 188 cm^{-1} can be assigned to heteropolar Sb-Se bond vibrations in $Sb(Se_{1/2})_3$ pyramidal structural units [22]. With the increase in indium content, the intensity of two dominant peaks at 188 and 250 cm^{-1} decreases and fades away for $x = 20$, 25 and favours the nucleation of new band at 212 cm^{-1} which is due to the vibrations of In and Se atoms. Also, with the increase in indium content, intensity of this dominant band increases [23]. The formation of stronger In-Se bonds as compared to Sb-Se bonds may thus favours the collapse of Se_8 rings or the broadening of the band to favour structural randomness in the network with disappearing of 188 cm^{-1} band with further increase in indium content [17].

3.3 Optical Properties

When EM-radiations, in the UV-VIS-NIR wavelength range interact with the sample, four phenomena are possible: the radiations may be transmitted, absorbed, reflected or scattered. Diffuse reflectance is an important tool which can be used for powdered, crystalline and nanostructure materials [25]. Figure 4 shows the spectral variation of the reflectance with wavelength for different powdered bulk samples. The absorption coefficient (α) were calculated using reflectance spectra by Kubelka-Munk equation [24]:

$$\alpha = \frac{K}{S} = \frac{(1-R)^2}{2R}$$

where, R is the absolute reflectance of the sample, K is molar absorption coefficient; S is the scattering coefficient and α is the absorption coefficient. Optical band gap of the samples was calculated by using Tauc plot equation as:

$$\alpha h\nu = B(h\nu - E_O)^n$$

where E_0 is the optical band gap, n is the constant that determines the type of various optical transitions i.e, $n = 1/2$ for direct allowed transition, $n = 2$ for indirect transitions and B is the parameter that depends upon the transition probability, the inverse of which is known as the tailing parameter describing the disorder in the network systems [26-28].

Figure 5 shows the plot of $(\alpha h\nu)^2$ versus hu for the $In_xSb_{30-x}Se_{70}$ ($0 \le x \le 25$) alloys. The values of optical band gap (E_0) and tailing parameter (B^{-1}) are determined from the intercept on energy axis with zero absorption and inverse of the slope, respectively. The calculated values of the E_0 and B^{-1} are summarized in Table 2. The addition of indium in host network of Sb-Se lead to the structural changes and hence optical band gap varies. It has been observed that the direct optical gap is 1.18 eV ($x = 0$) decreases to 1.05 eV ($x = 15$) and further increase in the concentration of additive results into an increase in the optical gap while the tailing parameter increases with the composition of the alloy. The decrease in band gap and corresponding increase in tailing parameter can be correlated with the chemical order of chalcogenide materials. The dominant contribution for states near the band edge of the chalcogenide alloys comes from their lone pair p-orbital [29]. The Pauling electronegativity (χ) values for In, Sb and Se is 1.78, 2.05 and 2.55 respectively [30]. Therefore, when the electronegative Sb atom is replaced by electropositive In atom then the energy of lone pair of electrons gets enhanced and hence,

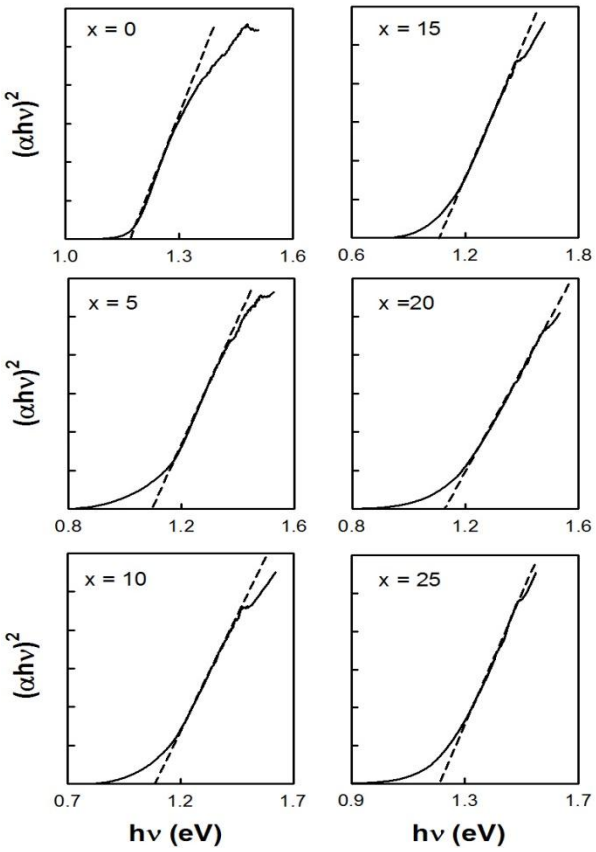

Fig. 5 – Tauc plots of $(\alpha h\nu)^2$ versus $h\nu$ for as-prepared bulk $In_xSb_{30-x}Se_{70}$ $(0 \le x \le 25)$ chalcogenide alloys

valence band move towards energy gap which leads to band tailing and hence decrease in energy band gap of the material [31]. Hence, the addition of more electropositive elements to the alloy may raise the energy level of lone pair states which are enough to broad the band inside forbidden gap. While the heterogeneous growth of crystalline phase may also augment the density of defect states, and disorder which is also associated with the decrease in band gap [26]. The optical properties can further be elaborated by using the chemically ordered covalent network model (COCNM), where the more strong bonds are favoured first and heteropolar bonds are favoured over the homopolar bonds. The bond energies for the probable bonds in this system viz. Se-Se, In-Se and Sb-Se are 44.02, 47.33 and 40.15 kcal/mol respectively [32]. Therefore, the iso valence substitution of Sb with In results into the increase in the average bond energy of the system and hence the increase in the optical gap at higher concentration of indium ($x = 20$, 25 at %) [33]. But, the sharp increase in the tailing parameter can be ascribed to increased disorder as evidenced by broadening of the Raman bands for the above said compositions.

4. CONCLUSIONS

Bulk samples were found polycrystalline with phases Sb_2Se_3 and β-In_2Se_3 as evidenced by XRD analysis. EDX analysis reveals that samples which we had prepared are nearly stoichiometric. Raman Spectra provides information about the characteristic vibrations of the isolated molecular units. $Sb_{30}Se_{70}$ exhibits five bands: two dominant peaks at 188 and 250 cm^{-1} and three weak peaks at ~ 112, 210, and 369 cm^{-1}.Broad band appear at 250 cm^{-1} is the manifestation of eight membered Se ring and at 188 cm^{-1}corresponds to heteropolar Sb-Se bond vibrations in $Sb(Se_{1/2})_3$ pyramidal structural units. Peaks at ~ 112 cm^{-1} and 369 cm^{-1} can be ascribed to the bond bending modes of the Se. The peak at ~ 210 cm^{-1} can be ascribed from either Se-Se chain bond or asymmetrical stretching of pyramidal $SbSe_3$ mode. As the increase in indium content, intensity of dominant peaks decreases and disappears for $x = 20$ and 25 and due to the vibrations of In and Se atoms, a dominant band is formed at 212 cm^{-1}. Also, due to heterogeneous growth of crystalline phases, band gap and tailing parameter were interpreted in terms of change in density of localized defect states and disorder. Correlation between electronegativity and band gap of the system also indicates that there is a decrease in direct band gap with the incorporation of In content. Further at high concentration of In, band gap increases because of increase in average bond energy.

AKNOWLEDGEMENTS

One of the author (SS) is thankful to the Department of Science and Technology, Govt. of INDIA, New Delhi [No. SR/S2/CMP- 0008/2011] for providing the financial assistance.

REFERENCES

1. A. Zakery, S.R. Elliott, *J. Non-Cryst. Solids* **330**, 1 (2003).
2. G. Lucovsky, F.L. Gleener, R.H. Geils, R.C. Keezer, *The Structure of Non Crystalline Materials* (Ed. by H. Gaskel) (Taylor and Francis: London: 1977).
3. S. Asokan, M.V.N. Prasad, G. Parthasarathy, E.S.R. Gopal, *Phys. Rev. Lett.* **62**, 808 (1989).
4. B. Effey, R.L. Cappelletti, *Phys. Rev. B* **59**, 4119 (1999).
5. M.F. Thorpe, *J. Non-Cryst. Solids* **57**, 355 (1983).
6. I. Watanabe, T. Yamamoto, *Jpn. J. Appl. Phys.* **24**, 1282 (1985).
7. I. Watanabe, T. Sekiya, *Jpn. J. Appl. Phys.* **26**, 663 (1987).
8. P. Kumar, R. Thangaraj, *J. Non-Cryst. Solids* **352**, 2288 (2006).
9. S.K. Srivastava, P.K. Dwivedi, A. Kumar, *Physica B* **183**, 409 (1993).
10. M.S. Iovu, E.P. Colomeico, I.A. Vasiliev, *Chal. Lett.* **4** (9), 109 (2007).
11. G. Kaur, T. Komatsu, *J. Mater Sci.* **36**, 4531 (2001).
12. Y.M. Yiu, T.K. Sham, G. Kaur, *J. Appl. Phys.* **104**, 013713 (2008).
13. S.R. Elliott, *Physics of Amorphous Materials* (Longman Scientific & Technical: John Wiley & Sons: New York: 1990).
14. Z.U. Borissova, *Glassy Semiconductors* (Plenum Press: New York: 1981).
15. M.A. Abdel-Rahim, M.M. Hafiz, A.M. Shamekh, *Physica B* **369**, F143 (2005).
16. A. Giridhar, S. Mahadevon, *J. Non-Cryst. Solids* **134**, 94 (1991).
17. J. Holubova, Z. Cernosek, E. Cernoskova, *J. Optoelectron.*

Adv. Mater. Rap. Comm. **1**, 663 (2007).
18. J. Schottmiller, M. Tabak, G. Lucovsky, T.A. Ward, *J. Non-Cryst. Solids* **4**, 80 (1970).
19. W. Richter, J.B. Rennuci, M. Cardona, *phys. status solidi b* **56**, 223 (1973).
20. N. Ohta, W. Scheuermann, K. Nakamoto, *Solid State Commun.* **27**, 1325 (1978).
21. A.B. Adam. *J. King. Saud University (Science)* **21**, 93 (2009).
22. R. Sharma, S. Sharma, P. Kumar, R. Chander, R. Thangaraj, M. Mian, *AIP Conf. Proc.* **1675**, 030041 (2015).
23. A.V. Kopytov, A.V. Kosobutsky, *Phys. Solid State* **51** No 10, 1994 (2009).
24. P. Kubelka, F. Munk, *Zeitschrift fur Technische Physik* **12**, 593 (1931).
25. http://www.piketech.com/technical/application-pdfs/Diffuse Theory&Appl.pdfS.
26. N.F. Mott, E.A. Davis, *Electronic Processes in Non-Crystalline Materials* (Clarendon: Oxford: 1979).
27. P. Kumar, R. Thangaraj, T.S. Sathiaraj, *phys. status solidi a* **208**, 838 (2011)
28. J. Tauc, *Amorphous and Liquid Semiconductors* (Plenum: New York: 1974).
29. M. Kastner, D. Adler, H. Fritzsche, *Phys. Rev. Lett.* **37**, 1504 (1976).
30. L. Pauling, *The Nature of Chemical Bond* (Cornell University: New York: 1976).
31. S. Sharda, N. Sharma, P. Sharma, V. Sharma, *Defects and Diffusion Forum* **45**, 316 (2011).
32. S. Sharma, R. Sharma, P. Kumar, R. Chander, R. Thangaraj, M. Mian, *AIP Conf. Proc.* **1675**, 030048 (2015).
33. A.K. Pattanaik, A. Srinivasan, *J. Optoelectron. Adv. Mater.* **5**, 1161 (2003).